# A comparison between Gaussian wavepacket dynamics of double-well systems in the Schrödinger and Heisenberg approaches

Hideo Hasegawa*

*Department of Physics, Tokyo Gakugei University, Koganei, Tokyo 184-8501, Japan*

(Dated: February 20, 2013)

## Abstract

Detailed numerical studies on Gaussian wavepacket dynamics in quantum systems with symmetric double-well (DW) potential have been made with the use of the two approaches: the Schrödinger approach (SA) and the Heisenberg approach combined with the time-dependent variational approximation (TDVA) to the Gaussian wavepacket method (GWM). We have calculated time dependences of wavefunctions, averages of position and momentum, the auto-correlation function and an uncertainty product. Our calculations show that a given initial Gaussian wavepacket in the SA is quickly deformed at $t > 0$ where a wavepacket cannot be expressed by a *single* Gaussian, and that assumptions on averages of higher-order fluctuations in TDVA are not justified in the SA. These results cast some doubt on an application of TDVA-GWM to double-well systems.

PACS numbers: 03.65.-w, 05.30.-d

*hideohasegawa@goo.jp

## I. INTRODUCTION

The time-dependent state of quantum systems may be described by the Schrödinger or Heisenberg approach [1]. In the Schrödinger approach (SA), the time-dependent wavefunction $\Psi(x,t)$ for the one-dimensional system is expressed by the partial differential equation

$$i\hbar \frac{\partial \Psi(x,t)}{\partial t} \;=\; H\Psi(x,t) = \left[-\frac{1}{2m}\frac{\partial^2}{\partial x^2} + U(x)\right]\Psi(x,t), \tag{1}$$

where notations are conventional. On the contrary, in the Heisenberg approach (HA), the dynamics of the system is described by equations of motion for operators $x$ and $p$

$$\frac{d\langle x\rangle}{dt} \;=\; \frac{\langle p\rangle}{m}, \quad \frac{d\langle p\rangle}{dt} = -\langle U'(x)\rangle, \tag{2}$$

where the bracket $\langle\cdot\rangle$ denotes an expectation value. It is generally difficult to obtain exact solutions for the Schrödinger and/or Heisenberg equations which are available only for limited cases like a harmonic oscillator (HO) system. Much efforts have been made to obtain approximate solutions for general quantum systems [1]. Although equations of motion given by Eq. (2) are closed within $\langle x\rangle$ and $\langle p\rangle$ for an HO system, they generally yield a hierarchy of equations of motion for higher-order fluctuations such as $\langle \delta x^2\rangle$, $\langle \delta p^2\rangle$ and $\langle \delta x\delta p + \delta p\delta x\rangle$ where $\delta x = x - \langle x\rangle$ and $\delta p = p - \langle p\rangle$.

The Gaussian wavepacket method (GWM) is one of such methods whose main aim is a semi-classical description of quantum systems (for a recent review on GWM, see Ref. [2]). If the wavefuction is Gaussian at $t = 0$ in an HO system, it remains at all $t > 0$. Heller [3] proposed to adopt a (thawed) Gaussian wavepacket given by

$$\Psi_H(x,t) \;=\; \exp\left[\frac{i}{\hbar}[A(x-\langle x\rangle)^2 + \langle p\rangle(x-\langle x\rangle) + \gamma]\right], \tag{3}$$

even for more realistic potentials, where $A$ and $\gamma$ are time-dependent complex parameters. Heller [3] derived equations of motion for $\langle x\rangle$, $\langle p\rangle$, $A$ and $\gamma$, employing an assumption that the potential expanded in the Taylor series at $x = \langle x\rangle$ may be truncated by

$$U(x) \;=\; U^{(0)}(\langle x\rangle) + U^{(1)}(\langle x\rangle)(x-\langle x\rangle) + \frac{1}{2}U^{(2)}(\langle x\rangle)(x-\langle x\rangle)^2. \tag{4}$$

The concept of the Gaussian wavepacket has been adopted in many fields [2]. Dynamics is well described by the GWM for an HO system where motions of fluctuations are separated from those of $\langle p\rangle$ and $\langle q\rangle$, and they lead to the uncertainty relation: $\langle \delta q^2\rangle\langle \delta p^2\rangle \geq \hbar^2/4$.

Various types of variants such as the frozen [4] and generalized Gaussian wavepacket methods [5] have been proposed [2]. Among them, we pay our attention to the time-dependent variational approximation (TDVA) which employs the normalized squeezed coherent-state Gaussian wavepacket given by [6–10]

$$\Psi_G(x,t) = \frac{1}{(2\pi\mu)^{1/4}} \exp\left[-\frac{(1-i\alpha)}{4\mu}(x-\langle x\rangle)^2 + i\,\frac{\langle p\rangle(x-\langle x\rangle))}{\hbar}\right], \tag{5}$$

$\mu$ and $\alpha$ being time-dependent parameters. For the introduced squeezed coherent state, Heisenberg equations of motion given by Eq. (2) are closed within $\langle x\rangle$, $\langle p\rangle$, $\langle \delta x^2\rangle$ and $\langle \delta x\delta p + \delta p\delta x\rangle$ [see Eqs. (33)-(36)]. A comparison between Heller's GWM and the TDVA is made in Refs. [9, 10].

There have been many studies on the GWP (including TDVA) which is applied to HO, anharmonic oscillator (AO) and Morse potentials [2]. The GWM has, however, some difficulty when applied to potentials including terms of $x^n$ with $n > 2$. Although it has been claimed that the GWM yields a fairly good result for AO systems [6], we wonder whether it actually works for double-well (DW) systems. DW potential models have been employed in a wide range of fields including physics, chemistry and biology (for a recent review on DW systems, see Ref. [11]). Lin and Ballentine [12], and Utermann, Dittrich and Hänggi [13] studied semi-classical properties of DW systems subjected to periodic external forces, calculating the Husimi function [14]. They show a chaotic behavior, in accordance with classical driven DW systems. Igarashi and Yamada [15] studied a coherent oscillation and decoherence induced by applied polychromatic forces in quantum DW system. By using the TDVA, Pattanayak and Schieve [8] pointed out that a chaos is induced by quantum noise in DW systems without external forces although classical counterparts are regular. This is in contrast to the usual expectation that quantum effects suppress classical chaos. Chaotic-like behavior was reported in a square DW system obtained by the exact SA calculation [16]. The validity of quantum chaos pointed out in Ref. [8] is still controversial [17–22].

The purpose of the present paper is twofold: to study dynamics of a given initial Gaussian wavepacket in DW systems with the use of both the SA and the HA combined with the TDVA, and to make a comparison between results of the two approaches. Such a study has not been reported as far as we aware of, and it is important to clarify significance of the TDVA-GWM applied to DW systems.

The paper is organized as follows. In Sec. II, we will mention the calculation method

employed in our study. We consider DW systems described by the symmetric DW (SDW) model. In solving the time-dependent Schrödinger equation, we have adopted the spectral method with energy matrix elements evaluated for a finite size $N_m$ (= 20 and 30). Our method is applied to SDW model in Sec. III, where we report time-dependences of the magnitude of wavefunction ($|\Psi(x,t)|^2$), an expectation value of $x$ ($\langle x\rangle$), the uncertainty product ($\langle\delta x^2\rangle\langle\delta p^2\rangle$) and the auto-correlation function ($C(t)$). In Sec. IV we apply our method also to an AO model. Sec. V is devoted to our conclusion.

## II. THE ADOPTED METHOD

### A. Schrödinger approach

We consider a quantum system whose Hamiltonian is given by

$$H \;=\; \frac{p^2}{2m} + U(x), \tag{6}$$

where $m$, $x$ and $p$ express a mass, position and momentum, respectively, of a particle and $U(x)$ stands for the DW potential. Various approximate analytical and numerical methods have been proposed to solve the Schrödinger equation given by Eq. (1) [1]. In our study we solve the Shrödinger equation, treating the Hamiltonian $H$ as

$$H \;=\; H_0 + U(x) - U_0(x) = H_0 + V(x), \tag{7}$$

with

$$H_0 \;=\; \frac{p^2}{2m} + U_0(x), \tag{8}$$

$$V(x) \;=\; U(x) - U_0(x). \tag{9}$$

Here $H_0$ denotes the Hamiltonian with an appropriate potential $U_0$, for which eigenfunction and eigenvalue are assumed to be given by $\phi_n(x)$ and $E_{0n}$, respectively.

For the stationary state, we expand the eigenfunction $\Psi(x)$ in terms of $\phi_n(x)$

$$\Psi(x) \;=\; \sum_{n=0}^{N_m} c_n \phi_n(x), \tag{10}$$

leading to the secular equation

$$Ec_m \;=\; \sum_{n=0}^{N_m} H_{mn} c_n, \tag{11}$$

where $E$ denotes the eigenvalue and $N_m$ is the maximum quantum number.

For the time-dependent state, we adopt a spectral method, expanding the eigenfunction $\Psi(x,t)$ in terms of $\phi_n(x)$

$$\Psi(x,t) \;=\; \sum_{n=0}^{N_m} c_n(t)\phi_n(x). \tag{12}$$

Time-dependent expansion coefficients $\{c_n(t)\}$ obey equations of motion given by

$$i\hbar\,\frac{\partial c_m(t)}{\partial t} \;=\; \sum_{n=0}^{N_m} H_{mn}\,c_n(t) \qquad (m=0 \text{ to } N_m), \tag{13}$$

with

$$H_{mn} \;=\; E_{0n}\,\delta_{m,n} + \int_{-\infty}^{\infty} \phi_m(x)^*\,V(x)\phi_n(x)\,dx. \tag{14}$$

Equation (13) expresses the $(N_m+1)$ first-order differential equation, which may be solved for a given initial condition of $\{c_n(0)\}$. Initial values of expansion coefficients $\{c_n(0)\}$ are determined by

$$c_n(0) \;=\; \int_{-\infty}^{\infty} \phi_n(x)^*\,\Psi_G(x,0)\,dx \qquad (n=0 \text{ to } N_m), \tag{15}$$

for a given initial Gaussian wavepacket $\Psi_G(x,0)$

$$\Psi_G(x,0) = \frac{1}{(2\pi\mu)^{1/4}}\,\exp\left[-\frac{(1-i\alpha)}{4\mu}(x-x_0)^2 + i\,\frac{p_0(x-x_0)}{\hbar}\right], \tag{16}$$

where $\mu$ and $\alpha$ are assumed parameters, and $x_0$ and $p_0$ are initial position and momentum, respectively, at $t=0$. Once solutions of $\{c_n(t)\}$ in Eq. (13) are obtained, the wavefunction $\Psi(x,t)$ may be constructed by Eq. (12).

In an alternative spectral method, the solution of the time-dependent Schrödinger equation may be expressed by

$$\Psi(x,t) \;=\; \sum_{\nu=0}^{N_m} a_\nu \Psi_\nu(x) e^{-iE_\nu t/\hbar}, \tag{17}$$

where $\Psi_\nu(x)$ and $E_\nu$ are eigenfunction and eigenvalue of the stationary state given by

$$H\Psi_\nu(x) \;=\; E_\nu\Psi_\nu(x) \qquad (\nu=0 \text{ to } N_m). \tag{18}$$

The time-independent expansion coefficient $a_\nu$ is determined by a given initial Gaussian wavepacket

$$a_\nu \;=\; \int_{-\infty}^{\infty} \Psi_\nu(x)^*\,\Psi_G(x,0)\,dx. \tag{19}$$

Both spectral methods given by Eqs. (12) and (17) yield the same results. The advantage of the former spectral method is that we may easily calculated the auto-correlation function and expectation values expressed in terms of $\{c_n(t)\}$ [see Eq. (54)-(59)], while the latter spectral method has clearer physical meaning. Model calculations to be reported in the following Sec. III have been made by using the former spectral method. Wavefunctions obtained by the spectral method have been cross-checked by the MATHEMATICA resolver for the partial differential equation.

### B. Heisenberg approach

It is possible to study dynamics of the quantum system with the use of the HA. Heisenberg equations of motion are expressed by [8–10]

$$\frac{d\langle x\rangle}{dt} = \frac{\langle p\rangle}{m}, \tag{20}$$

$$\frac{d\langle p\rangle}{dt} = -U'(\langle x\rangle) - \sum_{k=2}^{\infty} \frac{U^{(k+1)}(\langle x\rangle)}{k!}\langle \delta x^k\rangle, \tag{21}$$

$$\frac{d\langle \delta x^2\rangle}{dt} = \frac{1}{m}\langle \delta x\delta p + \delta p\delta x\rangle, \tag{22}$$

$$\frac{d\langle \delta x\delta p + \delta p\delta x\rangle}{dt} = -2\sum_{k=1}^{\infty} \frac{U^{(k+1)}(\langle x\rangle)}{k!}\langle \delta x^{k+1}\rangle + \frac{2}{m}\langle \delta p^2\rangle, \tag{23}$$

$$\frac{d\langle \delta p^2\rangle}{dt} = -\sum_{k=1}^{\infty} \frac{U^{(k+1)}(\langle x\rangle)}{k!}\langle \delta x^k\delta p + \delta p\delta x^k\rangle, \tag{24}$$

where $\delta p = p - \langle p\rangle$ and $\delta x = x - \langle x\rangle$. Equations (20)-(24) include high-order fluctuations which are not closed in general.

It is possible to construct various approximations depending on how many terms are taken into account in Eqs. (20)-(24). If we neglect the second term of Eq. (21), Eqs. (20) and (21) form classical equations of motion. When we neglect the second term in Eq. (21) and truncate Eqs. (23) and (24) at $k = 1$, Eqs. (20)-(24) reduce to equations of motion in Heller's Gaussian wavepacket approximation. Equations of motion including up to fourth-order corrections were obtained in Ref. [10].

One of conceivable ways to close equations of motion is to assume that a wavepacket is expressed by the normalized squeezed coherent state given by Eq. (5) [6, 8–10], which leads

to the relations

$$\langle \delta x^{2\ell} \rangle = \frac{(2\ell)!}{\ell!\, 2^\ell}\, \mu^\ell, \quad \langle \delta x^{2\ell+1} \rangle = 0, \quad (\ell = 1, 2, \cdot\cdot) \tag{25}$$

$$\langle \delta p^2 \rangle = \frac{\hbar^2 + \alpha^2}{4\mu}, \tag{26}$$

$$\langle \delta x \delta p + \delta p \delta x \rangle = \alpha, \tag{27}$$

$\mu$ and $\alpha$ being time-dependent parameters in the wavepacket. Equations (25)-(27) yield the uncertainty product

$$\langle \delta x^2 \rangle \langle \delta p^2 \rangle = \frac{\hbar^2 + \langle \delta x \delta p + \delta p \delta x \rangle^2}{4}. \tag{28}$$

From these relations, equations of motion given by Eqs. (20)-(24) become

$$\frac{d\langle x \rangle}{dt} = \frac{\langle p \rangle}{m}, \tag{29}$$

$$\frac{d\langle p \rangle}{dt} = -U'(\langle x \rangle) - \sum_{\ell=1}^{\infty} \frac{U^{(2\ell+1)}(\langle x \rangle)}{\ell!\, 2^\ell}\, \mu^\ell, \tag{30}$$

$$\frac{d\mu}{dt} = \alpha, \tag{31}$$

$$\frac{d\alpha}{dt} = \frac{\hbar^2 + \alpha^2}{2\mu} - \sum_{\ell=1}^{\infty} \frac{U^{(2\ell)}(\langle x \rangle)}{(\ell-1)!\, 2^{\ell-2}}\, \mu^\ell. \tag{32}$$

Alternatively, Eqs. (29)-(32) are rewritten as

$$\frac{d\langle x \rangle}{dt} = \frac{\langle p \rangle}{m}, \tag{33}$$

$$\frac{d\langle p \rangle}{dt} = -U'(\langle x \rangle) - \sum_{\ell=1}^{\infty} \frac{U^{(2\ell+1)}(\langle x \rangle)\langle \delta x^2 \rangle^\ell}{\ell!\, 2^\ell}, \tag{34}$$

$$\frac{d\langle \delta x^2 \rangle}{dt} = \frac{1}{m}\langle \delta x \delta p + \delta p \delta x \rangle, \tag{35}$$

$$\frac{d\langle \delta x \delta p + \delta p \delta x \rangle}{dt} = \frac{\hbar^2 + \langle \delta x \delta p + \delta p \delta x \rangle^2}{2m\langle \delta x^2 \rangle} - \sum_{\ell=1}^{\infty} \frac{U^{(2\ell)}(\langle x \rangle)\langle \delta x^2 \rangle^\ell}{(\ell-1)!\, 2^{\ell-2}}, \tag{36}$$

which are closed for $\langle x \rangle$, $\langle p \rangle$, $\langle \delta x^2 \rangle$ and $\langle \delta x \delta p + \delta p \delta x \rangle$.

By using a change of variables given by [6, 8, 9]

$$\rho^2 = \langle \delta q^2 \rangle, \tag{37}$$

$$\pi = \frac{1}{2\rho}\langle \delta q \delta p + \delta p \delta q \rangle, \tag{38}$$

Eqs. (29)-(32) are transformed to

$$\frac{d\langle q\rangle}{dt} = \frac{\langle p\rangle}{m}, \tag{39}$$

$$\frac{d\langle p\rangle}{dt} = -U'(\langle q\rangle) - \sum_{\ell=1}^{\infty} \frac{U^{(2\ell+1)}(\langle q\rangle)}{\ell!\, 2^{\ell}} \rho^{2\ell}, \tag{40}$$

$$\frac{d\rho}{dt} = \frac{\pi}{m}, \tag{41}$$

$$\frac{d\pi}{dt} = \frac{\hbar^2}{4\rho^3} - \sum_{\ell=1}^{\infty} \frac{U^{(2\ell)}(\langle q\rangle)}{(\ell-1)!\, 2^{\ell-1}} \rho^{2\ell-1}. \tag{42}$$

It was shown that fluctuation variables $\rho$ and $\pi$ are conjugate and that the effective Hamiltonian may be expressed in the extended phase space spanned by $\langle p\rangle$, $\langle q\rangle$, $\rho$ and $\pi$ [6, 8, 9]

$$H_{eff} = \frac{\langle p\rangle^2}{2m} + \frac{\pi^2}{2m} + \frac{\hbar^2}{8m\rho^2} + U(\langle q\rangle) + \sum_{\ell=1}^{\infty} \frac{U^{(2\ell)}}{\ell!\, 2^{\ell}} \rho^{2\ell}. \tag{43}$$

We should note that the effective Hamiltonian given by Eq. (43) relies on identities given by Eqs. (25)-(27) which are based on the assumed squeezed Gaussian wavepacket given by Eq. (5). If they are not held, the effective Hamiltonian given by Eq. (43) is not valid in DW systems: related discussion is given in Sec. V.

## III. MODEL CALCULATIONS

We apply our calculation method to the symmetric DW potential given by [23]

$$U(x) = \left(\frac{m\omega^2}{8x_s^2}\right) (x^2 - x_s^2)^2, \tag{44}$$

which has stable minima at $x = \pm x_s$ and an unstable maximum at $x_u = 0$ with the potential barrier of $\Delta = U(0) - U(\pm x_s) = m\omega^2 x_s^2/8$. As for $U_0(x)$, we adopt an HO potential given by

$$U_0(x) = \frac{m\omega^2 x^2}{2}, \tag{45}$$

where $\omega$ denotes the oscillator frequency. Eigenfunction and eigenvalue for $H_0$ are given by

$$\phi_n(x) = \frac{1}{\sqrt{2^n n!}} \left(\frac{m\omega}{\pi\hbar}\right)^{1/4} \exp\left(-\frac{m\omega x^2}{2\hbar}\right) H_n\left(\sqrt{\frac{m\omega}{\hbar}}\, x\right), \tag{46}$$

$$E_{0n} = \left(n + \frac{1}{2}\right)\hbar\omega \qquad (n = 0, 1, 2\cdot, \cdots), \tag{47}$$

where $H_n(x)$ stands for the Hermite polynomials.

Matrix elements $H_{mn}$ in Eq. (14) are given as follows: We rewrite the potential $U(x)$ as

$$U(x) \;=\; \frac{A_4 x^4}{4} + \frac{A_3 x^3}{3} + \frac{A_2 x^2}{2} + A_1 x + A_0, \tag{48}$$

with

$$A_4 \;=\; \frac{m\omega^2}{2d^2}, \;\; A_3 = 0, \;\; A_2 = -\frac{m\omega^2}{2}, \;\; A_1 = 0, \;\; A_0 = \frac{m\omega^2 d^2}{8}. \tag{49}$$

By using relations given by

$$q \;=\; \sqrt{\frac{g}{2}}(a^\dagger + a), \quad p = i\frac{\hbar}{\sqrt{2g}}(a^\dagger - a), \qquad \left(g = \tfrac{\hbar}{m\omega}\right) \tag{50}$$

$$a^\dagger\,\phi_n \;=\; \sqrt{n+1}\,\phi_{n+1}, \;\; a\,\phi_n = \sqrt{n}\,\phi_{n-1}, \tag{51}$$

we obtain the symmetric matrix elements $H_{mn}$ for $m \le n$ given by

$$\begin{aligned}
H_{mn} \;=\; & \left[(n+1/2)\,\hbar\omega + \frac{3A_4 g^2}{16}(2n^2+2n+1) + \frac{A_2'\,g}{2}(n+1/2) + A_0\right]\,\delta_{m,n} \\
+ \; & \left[A_3\left(\frac{g}{2}\right)^{3/2} n\sqrt{n} + A_1\left(\frac{g}{2}\right)^{1/2}\sqrt{n}\right]\delta_{m,n-1} \\
+ \; & \left[\frac{A_4 g^2}{8}(n-1)\sqrt{n(n-1)} + \frac{A_2'\,g}{4}\sqrt{n(n-1)}\right]\,\delta_{m,n-2} \\
+ \; & \frac{A_3}{3}\left(\frac{g}{2}\right)^{3/2}\sqrt{n(n-1)(n-2)}\,\delta_{m,n-3} \\
+ \; & \frac{A_4 g^2}{16}\sqrt{n(n-1)(n-2)(n-3)}\,\delta_{m,n-4},
\end{aligned} \tag{52}$$

where $A_2' = A_2 - m\omega^2$.

Various time-dependent quantities may be expressed in terms of $\{c_n(t)\}$ as follows: After some manipulations with the use of the relations given by Eqs.(50) and (51), the auto-correlation function is given by

$$C(t) \;=\; \int_{-\infty}^{\infty} \Psi(x,t)^*\Psi(x,0)\,dx, \tag{53}$$

$$\;=\; \sum_{n=0}^{N_m} c_n(t)^*\,c_n(0), \tag{54}$$

and expectation values of $x(t)$ and $p(t)$ are expressed by

$$\langle x(t)\rangle = \sqrt{\frac{g}{2}}\sum_n \left[\sqrt{n+1}\, c^*_{n+1}(t)c_n(t) + \sqrt{n}\, c^*_{n-1}(t)c_n(t)\right], \tag{55}$$

$$\langle p(t)\rangle = i\sqrt{\frac{\hbar^2}{2g}}\sum_n \left[\sqrt{n+1}\, c^*_{n+1}(t)c_n(t) - \sqrt{n}\, c^*_{n-1}(t)c_n(t)\right], \tag{56}$$

$$\begin{aligned}\langle x(t)^2\rangle &= \left(\frac{g}{2}\right)\sum_n [\sqrt{(n+1)(n+2)}\, c^*_{n+2}(t)c_n(t) + (2n+1)\, c^*_n(t)c_n(t) \\ &+ \sqrt{n(n-1)}\, c^*_{n-2}(t)c_n(t)],\end{aligned} \tag{57}$$

$$\begin{aligned}\langle p(t)^2\rangle &= -\left(\frac{\hbar^2}{2g}\right)\sum_n [\sqrt{(n+1)(n+2)}\, c^*_{n+2}(t)c_n(t) - (2n+1)\, c^*_n(t)c_n(t) \\ &+ \sqrt{n(n-1)}\, c^*_{n-2}(t)c_n(t)],\end{aligned} \tag{58}$$

$$\begin{aligned}\langle x(t)p(x) + p(t)x(t)\rangle &= i\,\hbar\sum_n [\sqrt{(n+1)(n+2)}\, c^*_{n+2}(t)c_n(t) \\ &- \sqrt{n(n-1)}\, c^*_{n-2}(t)c_n(t)].\end{aligned} \tag{59}$$

Figure 1 expresses the adopted quartic DW potential $U(x)$ with $x_s = 2\sqrt{2}$ and $\Delta = 1.0$

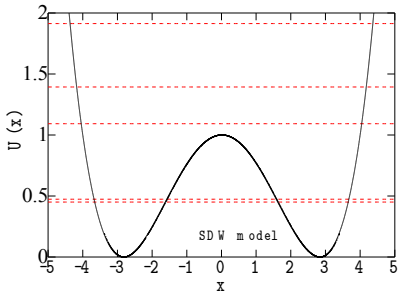


FIG. 1: (Color online) The symmetric DW potential (solid curve) with $x_s = 2\sqrt{2}$ and $\Delta = 1.0$ in Eq. (44), dashed curves expressing eigenvalues of $E_\nu$ ($\nu = 0 - 4$).

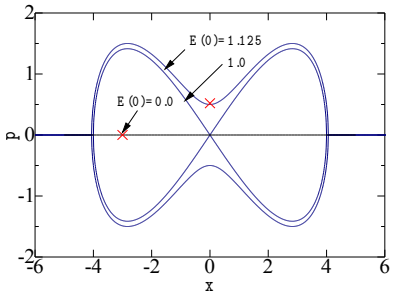


FIG. 2: (Color online) The classical $x$-$p$ phase space of the SDW model for various initial energies ($E(0)$), marks $\times$ denoting positions of initial states adopted in our calculations.

in Eq. (44). We have calculated energy matrix elements of $H_{mn}$, by using Eq. (52) with $m = 1.0$, $\omega = 1.0$, $\hbar = 1.0$ and $N_m = 30$. Obtained eigenvalues are $E_\nu = 0.450203$, 0.474126, 1.09262, 1.39334 and 1.91286 for $\nu = 0$ to 4, respectively, which are plotted by dashed curves in Fig. 1. The ground state ($E_0$) and first excited state ($E_1$), which are quasi-degenerate, are below the potential barrier of $\Delta = 1.0$. The energy gap between $E_0$ and $E_1$ is $\delta = 0.023923$. Low-lying eigenvalues calculated with $N_m = 30$ are in good agreement with those obtained with $N_m = 20$.

Figure 2 shows the classical $x$-$p$ phase space for initial energies of $E(0) = 0.0$, 1.0 and 1.125. Marks $\times$ in Fig. 2 show two kinds of initial states in the $x - p$ phase space: (1) $(x_0, p_0) = (-2\sqrt{2}, 0.0)$ and (2) $(x_0, p_0) = (0.0, 0.5)$. Calculated results for the two initial states (1) and (2) will be separately reported in the following.

*1. Case of the initial state of* $(x_0, p_0) = (-2\sqrt{2}, 0.0)$

We have adopted the initial Gaussian wavepacket $\Psi_G(x)$ locating at the stable point of the left well with $(x_0, p_0) = (-2\sqrt{2}, 0.0)$, $\mu = 0.1$ and $\alpha = 0.0$, which yields the minimum uncertainty product of $\langle \delta x^2 \rangle \langle \delta p^2 \rangle = 1/4$ at $t = 0.0$. A norm of the initial Gaussian wavepacket is $\sum_n c_n(0)^* c_n(0) = 0.999999$. Initial coefficients $\{c_n(0)\}$ calculated by Eq. (15) are real with appreciable magnitudes at $3 \lesssim n \lesssim 10$. After solving $(N_m + 1)$ first-order differential equations for $\{c_n(t)\}$ given by Eq. (13) for initial values of $\{c_n(0)\}$, we obtain the time-dependent eigenfunction $\Psi(x, t)$ expressed in terms of $\{c_n(t)\}$ in Eq. (12).

Figure 3 shows the 3D plot of $|\Psi(x, t)|^2$ calculated by the SA. We note that the initial Gaussian wavepacket in the SA is quickly spread as the time develops. In order to scrutinize the behavior of $|\Psi(x, t)|^2$ at small $t$, its time dependence at $0 \leq t \leq 25$ is plotted by bold solid curves in Fig. 4, where solid curves denote results of the TDVA. The Gaussian wavepacket at $t = 0.0$ in the SA is widespread even at $t = 5.0$, and its trend becomes more significant with increasing $t$. Figure 3 clearly shows that $|\Psi(x, t)|^2$ in the SA is quite different from that in the TDVA and that $\Psi(x, t)$ cannot be expressed by a single Gaussian wavepacket except at $t = 0.0$.

The difference between the SA and TDVA is more clearly seen in the time-dependent expectation value of $\langle x \rangle$. Figure 5(a) shows $\langle x \rangle$ of the SA, which expresses a tunneling of a particle oscillating with the period of about 260, which is consistent with the period estimated from the energy gap by $T = 2\pi/\delta = 262$. On the contrary, $\langle x \rangle$ of the TDVA in Figs. 5(b) shows more rapid oscillation with a period of about $25 - 30$.

Figures 6(a) and 6(b) show $\langle x \rangle$ vs. $\langle p \rangle$ plots calculated by the SA and TDVA, respectively. The $\langle x \rangle$ vs. $\langle p \rangle$ plot of the SA in Fig. 6(a) is quite different from that of the TDVA in Fig. 6(b).

Figure 7(a) shows the uncertain product of $\langle \delta x^2 \rangle \langle \delta p^2 \rangle$ calculated by the SA, which expresses a measure of quantum fluctuation. It starts from the minimum uncertainty of $1/4$ at $t = 0$, and with increasing $t$ it grows and oscillates between about 5 and 17 with the period of about 130. For a comparison, we plot $(1 + \langle \delta x \delta p + \delta x \delta p \rangle^2)/4$ in Fig. 7(b). In the TDVA, both the quantities agree as expressed in Eq. (28). Figures 7(a) and 7(b) show that this equality is not satisfied in the SA.

Figures 8(a) and 8(a) show the auto-correlation functions $|C(t)|^2$ calculated by the SA

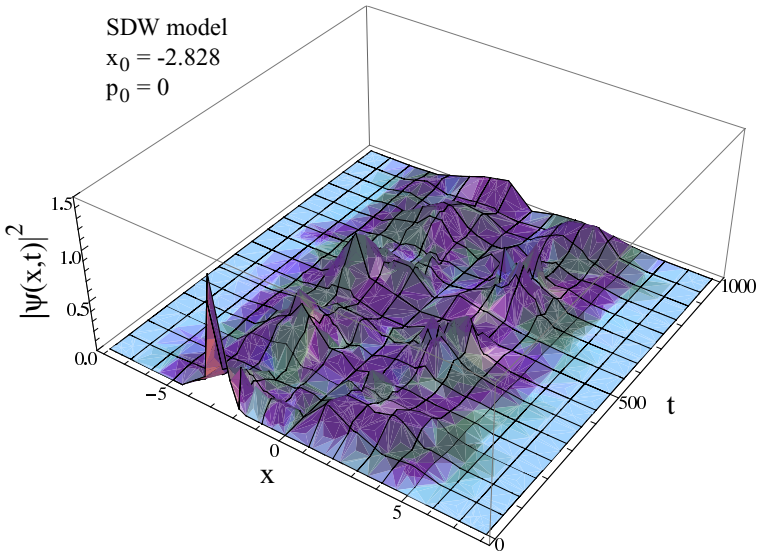


FIG. 3: (Color online) 3D plot of $|\Psi(x,t)|^2$ as functions of $x$ and $t$ of the symmetric model $(x_0 = -2\sqrt{2}, p_0 = 0.0)$.

and the TDVA, respectively, with Eq. (54). $|C(t)|^2$ of the SA which is unity at $t = 0.0$, oscillates between about 0.1 and 0.7 with a period of about 260, same as that of $\langle x \rangle$ shown in Fig. 5(a). The result of the TDVA is again rather different from that of the SA.

*2. Case of the initial state of* $(x_0, p_0) = (0.0, 0, 5)$

Next we adopt a different initial Gaussian wavepacket locating at $(x_0, p_0) = (0.0, 0.5)$ with $\mu = 0.1$ and $\alpha = 0.0$, for which the initial energy is $E(0) = 1.125$ (see Fig. 2). Initial coefficients $\{c_n(0)\}$ calculated by Eq. (15) are complex with appreciable magnitudes at

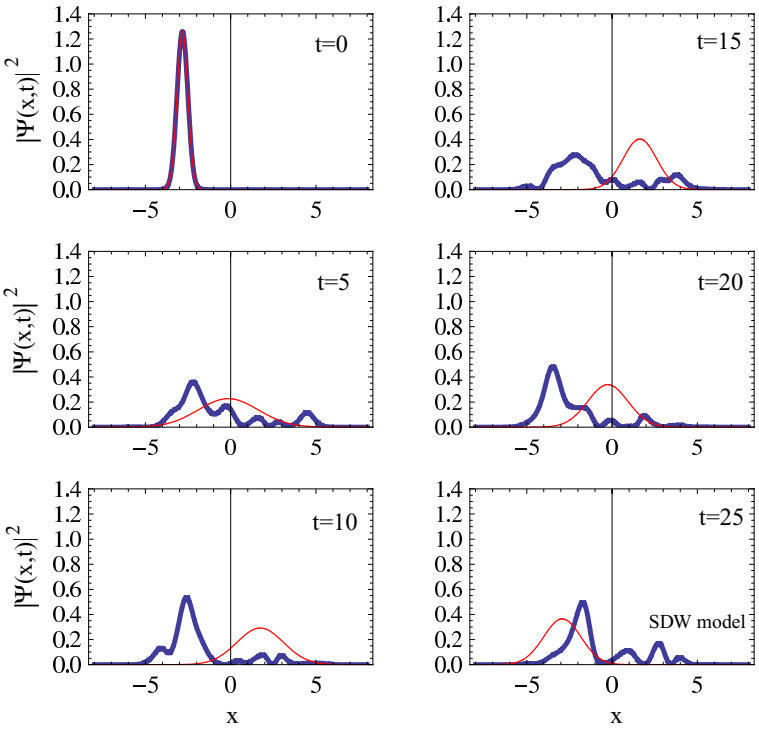


FIG. 4: (Color online) The $x$ dependence of $|\Psi(x,t)|^2$ at various $t$ of the SDW model calculated by the SA (bold solid curves) and the TDVA (solid curve) ($x_0 = -2\sqrt{2}, p_0 = 0.0$).

$0 \lesssim n \lesssim 15$. The initial state of $(x_0, p_0) = (0.0, 0, 5)$ locates near a top of the potential barrier (see Fig. 2). Note that in the classical calculation, the $x$ vs. $p$ plot forms a cocoon shape extending from $x = -4.06021$ to $x = 4.06021$ and from $p = -1.5$ to 1.5, as shown in Fig. 2. Then at $t > 0$, a classical particle rolls down the potential up to $x = 4.06021$ and approaches $x = -4.06021$ after passing through $x = 0$ in the classical calculation. However, this classical behavior is quite different from quantum results calculated by the SA and TDVA. The 3D plot of $|\Psi(x,t)|^2$ of the SA shown in Fig. 9 has an appreciable magnitude at $-5 \lesssim x \lesssim 5$. Bold solid curves and solid curves in Fig. 10 show $|\Psi(x,t)|^2$ calculated by the SA and the TDVA, respectively. $|\Psi(x,t)|^2$ in the SA is distorted and widespreads at $t > 0$,

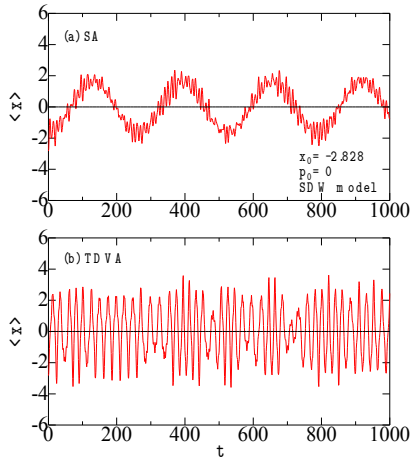


FIG. 5: (Color online) The time dependence of $\langle x \rangle$ of the symmetric model calculated by (a) the SA and (b) the TDVA ($x_0 = -2\sqrt{2}, p_0 = 0.0$).

which is different from the relevant result of the TDVA. An expectation value of $\langle x \rangle$ of the SA in Fig. 11(a) does not so much depart from the initial point of $x = 0.0$ in contrast to that of the TDVA shown in Fig. 11(b).

The $\langle x \rangle$ vs. $\langle p \rangle$ plots calculated by the SA and TDVA are shown in Figs. 12(a) and 12(a), respectively. The result of the SA in Fig. 12(a) shows a chaotic-like motion, which is different from a quasi-periodic motion of the TDVA in Fig. 12(b).

Figure 13(a) and 13(b) shows SA calculations of $\langle \delta x^2 \rangle \langle \delta p^2 \rangle$ and $(1 + \langle \delta x \delta p + \delta x \delta p \rangle^2)/4$, respectively. The TDVA yields that the former quantity is equal to the latter, which is not realized in the SA.

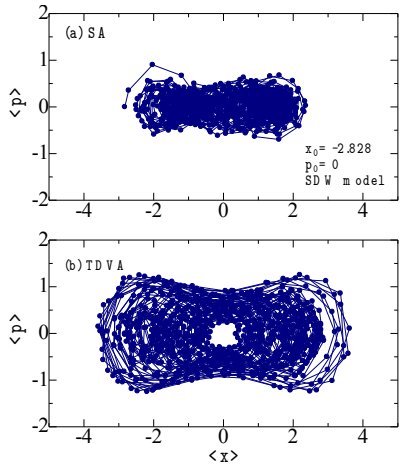


FIG. 6: (Color online) The $\langle x\rangle$ vs. $\langle p\rangle$ plots of the symmetric model calculated by (a) the SA and (b) the TDVA, time step being $\Delta t = 1.0$ ($x_0 = -2\sqrt{2}, p_0 = 0.0$).

## IV. DISCUSSION

We have studied Gaussian wavepacket dynamics of quantum DW systems in the preceding section. It is worthwhile to examine also an AO model given by

$$U(x) \;=\; \frac{x^2}{2} + \frac{bx^4}{4} = U_0(x) + \frac{bx^4}{4}, \tag{60}$$

where $b$ expresses a degree of anharmonicity. We have repeated calculations, by using the method mentioned in Sec. II with necessary modifications.

Figure 14(a) shows the 3D plot of $|\Psi(x,t)|^2$ for $b = 0.01$ with an assumed initial Gaussian state for $(x_0, p_0) = (-1.0, 0.0)$, $\mu = 0.1$ and $\alpha = 0.0$. In the case of the HO ($b = 0.0$), $|\Psi(x,t)|^2$ is periodic with a period of $T_0 = 2\pi/\omega$. Figure 14(a) shows that $|\Psi(x,t)|^2$ for a small $b = 0.01$ is nearly periodic as that for $b = 0.0$ at $t < 10$. For a larger $b = 0.1$, however, this periodicity is destroyed and the wavepacket spreads in the non-Gaussian form as Fig. 14(b) shows. This is more clearly realized in the $x$-dependence of $|\Psi(x,t)|^2$ for the SA plotted by bold solid curves in Fig. 15, which are different from those of the TDVA

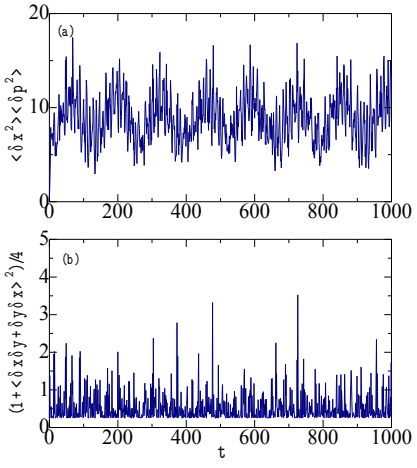


FIG. 7: (Color online) Time dependence of (a) the uncertainty product: $\langle \delta x^2 \rangle \langle \delta p^2 \rangle$ and (b) $(1 + \langle \delta x \delta p + \delta x \delta p \rangle^2)/4$ of the symmetric model calculated by the SA ($x_0 = -2\sqrt{2}, p_0 = 0.0$). Note that $\langle \delta x^2 \rangle \langle \delta p^2 \rangle$ equals to $(1 + \langle \delta x \delta p + \delta x \delta p \rangle^2)/4$ in the TDVA [Eq. (28)], which is not realized in (a) and (b).

shown by solid curves. Our result of the SA in Fig. 15 is consistent with that in Ref. [24] which studies effects of anharmonicity and interactions in DW systems.

Figure 16(a) and 16(a) show time dependences of $\langle x \rangle$ calculated by the SA and TDVA, respectively. $\langle x \rangle$ oscillates with a period of about 5.6 in both results. However, a period of its envelope variation in the SA ($\sim 110$) is larger than that in the TDVA ($\sim 30$): the former corresponds to the revival time after which a wavepacket periodically returns to the initial shape.

## V. CONCLUSION

By using the SA and HA combined with the TDVA, we have numerically studied dynamics of Gaussian wavepackets in quantum DW systems with the symmetric quartic potential. A

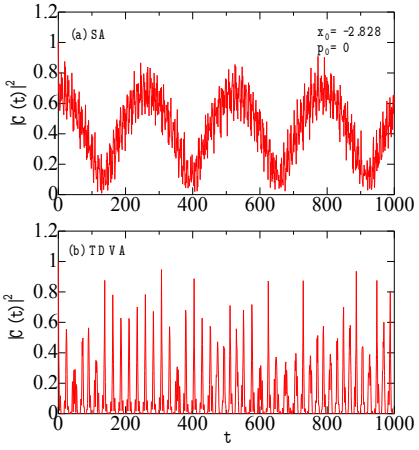


FIG. 8: (Color online) Time dependences of the auto-correlation function $|C(t)|^2$ of the symmetric DW model calculated by (a) the SA and (b) the TDVA ($x_0 = -2\sqrt{2}, p_0 = 0.0$).

comparison between calculated results of the SA and TDVA-GWM has shown the following:

(1) With time developing, a given initial Gaussian wavepacket of the SA spreads and deforms in symmetric DW system where a wavepacket at $t > 0$ cannot be expressed by a single Gaussian,

(2) Time dependences of expectation values of $\langle x \rangle$ and $\langle p \rangle$ and the auto-correlation function $C(t)$ in the TDVA are rather different from their counterparts in the SA, and

(3) The relation for uncertainty product given by Eq. (28) derived in the TDVA is not satisfied in the SA.

The item (1) which holds also in asymmetric DW systems [26], is in contrast to the postulate expressed by Eq. (3) or Eq. (5) in the GWM. Items (2) and (3) suggest that TDVA cannot be a good approximation for DW systems, which throws doubt on studies having been made with the use of the TDVA. It might be possible that the effective Hamiltonian in the extended phase space given by Eq. (43) cannot be applied to DW systems because it is derived with the assumed squeezed Gaussian wavepacket given by Eq. (5) in TDVA.

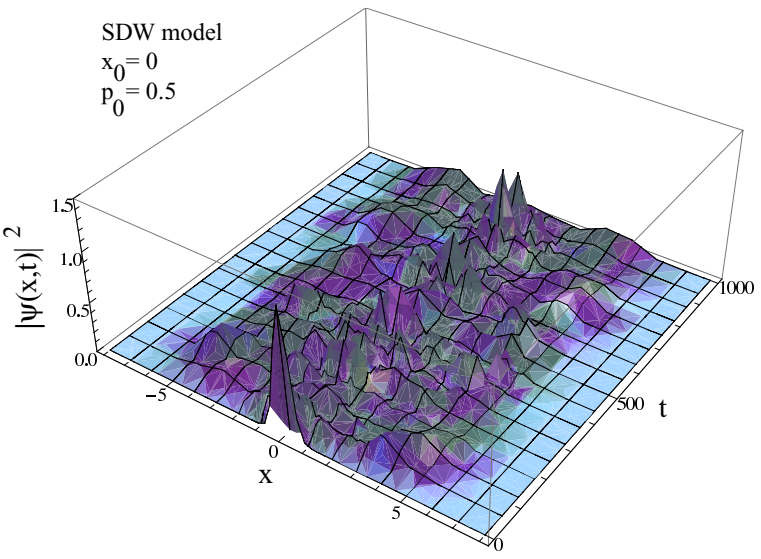


FIG. 9: (Color online) 3D plot of $|\Psi(x,t)|^2$ as functions of $x$ and $t$ of the symmetric DW model ($x_0 = 0.0, p_0 = 0.5$).

Nevertheless, quantum chaos in DW systems first pointed out Pattanayak and Schieve [8] by using the TDVA, is supported by our SA calculation, which is consistent with Ref. [16]. The GWM provides us with an efficient and physically-transparent calculation method, clarifying the relation between quantum and classical mechanics. The GWM is considered to be best applied to dynamics in HO and AO with a small anharmonicity. For a better description of quantum DW systems, it might be necessary to adopt extended GWMs with superimposed multiple Gaussian wavepackets (see Ref. [25], related references therein), which are much sophisticated and complicated than the original Heller's GWM [3].

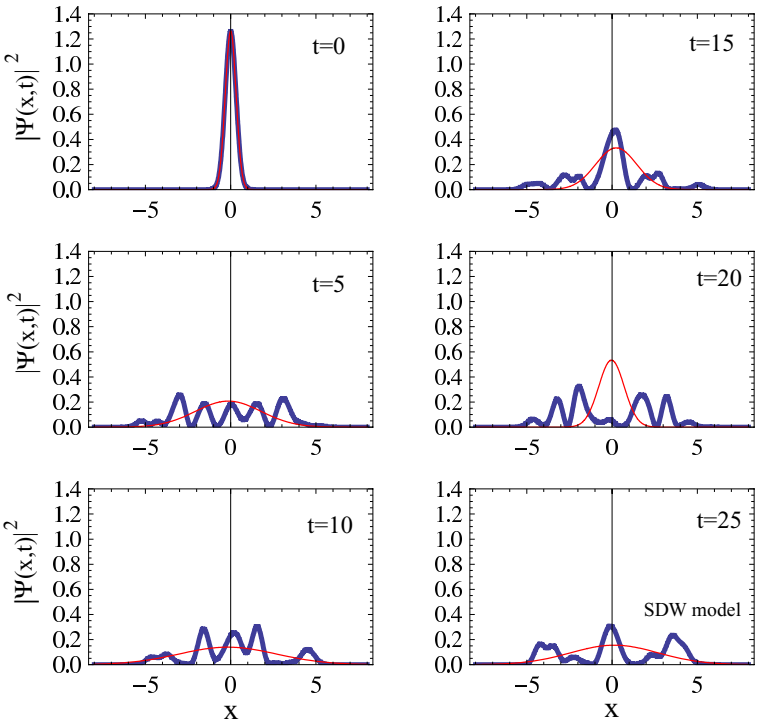


FIG. 10: (Color online) The $x$ dependence of $|\Psi(x,t)|^2$ at various $t$ of the SDW model calculated by the SA (bold solid curves) and the TDVA (solid curves) ($x_0 = 0.0, p_0 = 0.5$).

**Acknowledgments**

This work is partly supported by a Grant-in-Aid for Scientific Research from Ministry of Education, Culture, Sports, Science and Technology of Japan.

---

[1] D. J. Tannor, *Introduction to quantum mechanics: A time-dependent perspective* (Univ. Sci. Books, Sausalito, California, 2007).

[2] R.W. Robinett, Phys. Rep. **392**, 1 (2004).

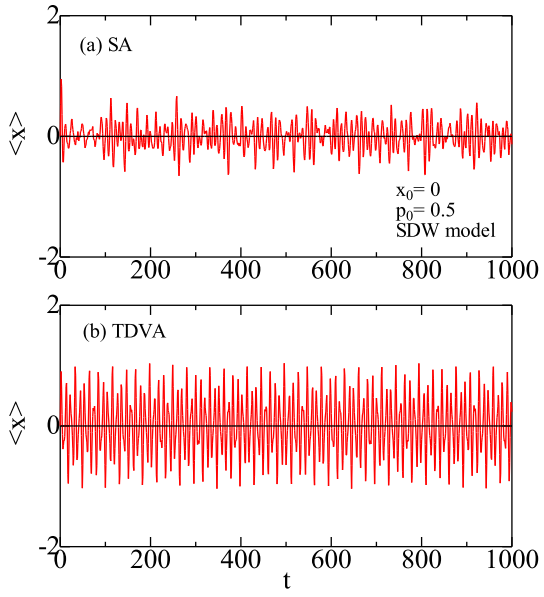


FIG. 11: (Color online) The time dependence of $\langle x \rangle$ of the symmetric DW model calculated by (a) the SA and (b) the TDVA ($x_0 = 0.0, p_0 = 0.5$).

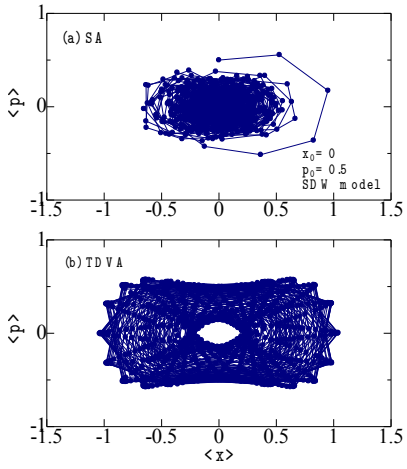


FIG. 12: (Color online) The $\langle x \rangle$ vs. $\langle p \rangle$ plots of the symmetric DW model calculated by (a) the SA and (b) the TDVA, time step being $\Delta t = 1.0$ ($x_0 = 0.0, p_0 = 0.5$).

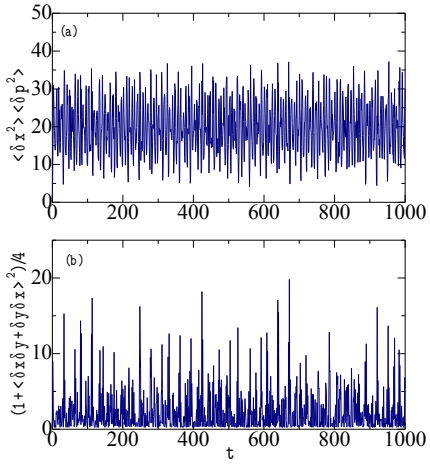


FIG. 13: (Color online) Time dependence of (a) the uncertainty product: $\langle \delta x^2 \rangle \langle \delta p^2 \rangle$ and (b) $(1 + \langle \delta x \delta p + \delta x \delta p \rangle^2)/4$ of the symmetric DW model calculated by the SA ($x_0 = 0.0, p_0 = 0.5$). Note that $\langle \delta x^2 \rangle \langle \delta p^2 \rangle$ equals to $(1 + \langle \delta x \delta p + \delta x \delta p \rangle^2)/4$ in the TDVA [Eq. (28)], which is not realized in (a) and (b).


[3] E. J. Heller, J. Chem. Phys. **62**, 1544 (1975).

[4] E. J. Heller, J. Chem. Phys. **75**, 2923 (1981).

[5] D. Huber and E. J. Heller, J. Chem. Phys. **87**, 5302 (1987).

[6] F. Cooper, S.-Y. Pi, and P. N. Stancioff, Phys. Rev. D **34**, 3831 (1986).

[7] Y. Tsue and Y. Fujiwara, Prog. Theo. Phys. **86**, 443 (1991).

[8] A. K. Pattanayak and W. C. Schieve, Phys. Rev. Lett. **72**, 2855 (1994).

[9] A. K. Pattanayak and W. C. Schieve, Phys. Rev. E **50**, 3601 (1994).

[10] B. Sundaram and P. W. Milonni, Phys. Rev. E **51**, 1971 (1995).

[11] M. Thorwart, M. Grifoni, and P. Hänggi, Annals Phys. **293**, 14 (2001).

[12] W. A. Lin, L. E. Ballentine, Phys. Rev. Lett. **65**, 2927 (1990); Phys. Rev. A **45**, 3637 (1992).

[13] R. Utermann, T. Dittrich, and P. Hänggi, Phys. Rev. E **49**, 273 (1994).

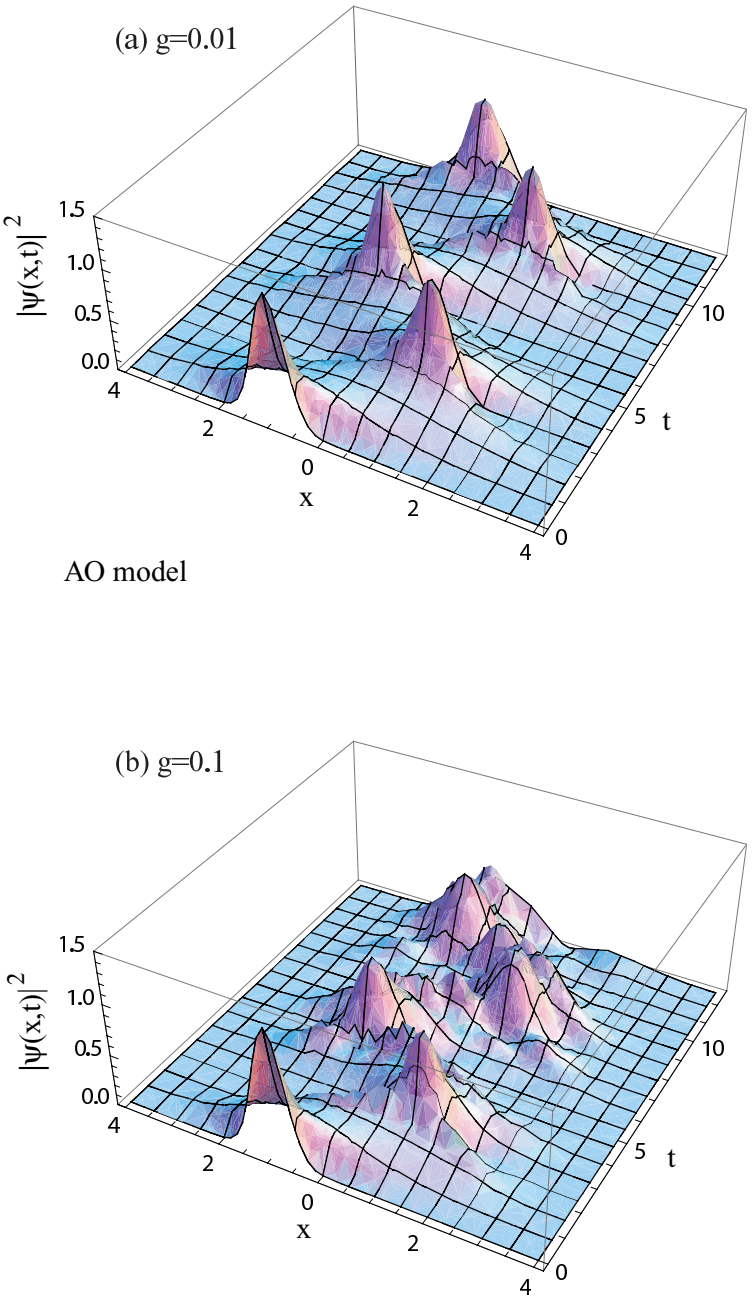


FIG. 14: (Color online) 3D plot of $|\Psi(x,t)|^2$ as functions of $x$ and $t$ with (a) $b = 0.01$ and (b) $b = 0.1$ of the AO model ($x_0 = -1.0, p_0 = 0.0$).

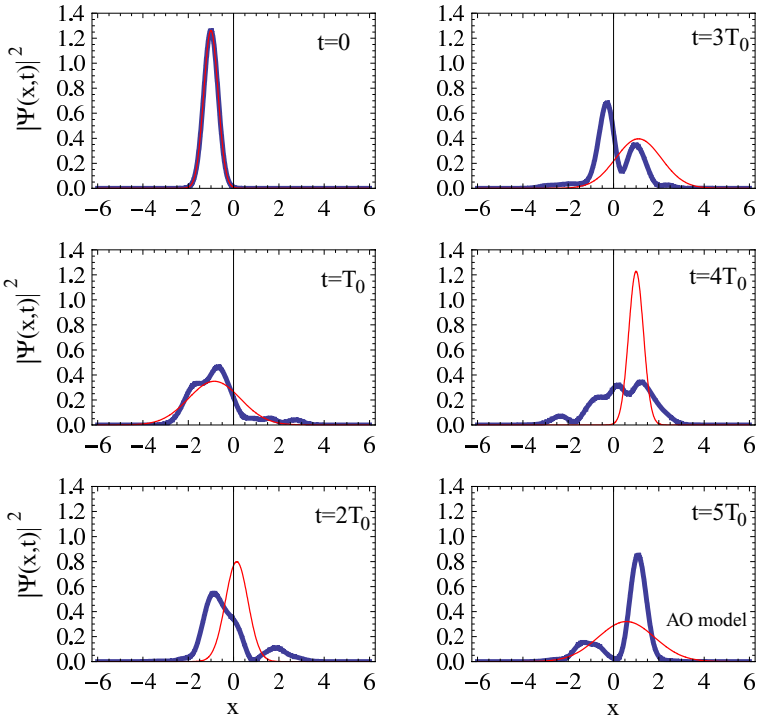


FIG. 15: (Color online) The $x$ dependence of $|\Psi(x,t)|^2$ at $t = kT_0$ $(k = 0, 1, 2\cdots)$ for the AO model with $b = 0.1$ calculated by the SA (bold solid curves) and the TDVA (solid curve) $(x_0 = -1.0, p_0 = 0.0)$, where $T_0$ $(= 2\pi/\omega)$ is a period for $b = 0$ (HO).


[14] K. Husimi, Proc. Phys. Math. Soc. Jpn. **22**, 264 (1940).

[15] A. Igarashi, and H. Yamada, Physica D **221**, 146 (2006).

[16] Y. Ashkenazy, L. P. Horwitz, J. Levitan, M. Lewkowicz, and Y. Rothschild, Phys. Rev. Lett. **75**, 1070 (1995).

[17] A. K. Pattanayak and W. C. Schieve, Phys. Rev. A **54**, 947 (1996).

[18] T. C. Blum and Hans-Thomas Elze, Phys. Rev. E **53**, 3123 (1996).

[19] O. F. de Alcantara Bonfim, J. Florencio and F. C. Sa Barreto, Phys. Rev. E **58**, 6851 (1998).

[20] B. C. Bag and D. S. Ray, Phys. Rev. E **61**, 3223 (2000).

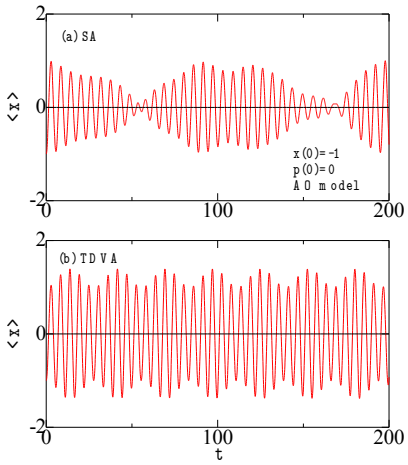


FIG. 16: (Color online) The time dependence of $\langle x \rangle$ in the AO model with $b = 0.1$ calculated by (a) the SA and (b) the TDVA ($x_0 = -1.0, p_0 = 0.0$).

[21] A. Roy and J. K. Bhattacharjee, Phys. Letters A **288**, 1 (2001).

[22] S. Habib, arXiv:0406011.

[23] H. Hasegawa, Phys. Rev. E **86**, 061104 (2012).

[24] M. Herrera, T. M. Antonsen, E. Ott, and S. Fishman, arXiv:1212.2850.

[25] J. O. Zoppe, M. L. Parkinson, M. Messina, Chem. Phys. Lett. **407**, 308 (2005).

[26] H. Hasegawa, arXiv:1302.4110.